Published in final edited form as:
Sci Transl Med. 2014 July 9; 6(244): 244re5. doi:10.1126/scitranslmed.3008882.

Plasmodium falciparum transmission stages accumulate in the human bone marrow

Regina Joice[1], **Sandra K. Nilsson**[1,*], **Jacqui Montgomery**[2,3,*], **Selasi Dankwa**[1], **Elizabeth Egan**[1], **Belinda Morahan**[4], **Karl B. Seydel**[5,6], **Lucia Bertuccini**[7], **Pietro Alano**[7], **Kim C. Williamson**[4], **Manoj T. Duraisingh**[1], **Terrie E. Taylor**[5,6], **Danny A. Milner**[1,5,8], and **Matthias Marti**[1,†]

[1]Department of Immunology and Infectious Diseases, Harvard School of Public Health, 665 Huntington Avenue, Boston, MA 02115, USA

[2]Malawi-Liverpool-Wellcome Trust Clinical Research Programme, P. O. Box 30096, Chichiri, Blantyre 3, Malawi

[3]Liverpool School of Tropical Medicine, University of Liverpool, Liverpool L3 5QA, UK

[4]Department of Biology, Loyola University, 1032 West Sheridan Road, Chicago, IL 60660, USA

[5]Blantyre Malaria Project, University of Malawi College of Medicine, Blantyre 3, Malawi

[6]College of Osteopathic Medicine, Michigan State University, East Lansing, MI 48824, USA

[7]Dipartimento di Malattie Infettive, Parassitarie ed Immunomediate, Istituto Superiore di Sanita, Viale Regina Elena n. 299, 00191 Rome, Italy

[8]Department of Pathology, Brigham and Women's Hospital, 75 Francis Street, Boston, MA 02115, USA

†Corresponding author. mmarti@hsph.harvard.edu.
*These authors contributed equally to this work.

Competing interests: The authors declare that they have no competing interests.

SUPPLEMENTARY MATERIALS
www.sciencetranslationalmedicine.org/cgi/content/full/6/244/244re5/DC1
Materials and methods
Fig. S1. Representative pLDH and Pfs16 labeling across tissues.
Fig. S2. Stage specificity of antibodies by immunohistochemistry.
Fig. S3. Morphology and dimensions of parasites by immunohistochemistry.
Fig. S4. Development of qRT-PCR assay.
Fig. S5. RNA quality from brain and bone marrow tissue samples.
Fig. S6. Invasion and development of gametocytes in erythroid precursor cells.
Fig. S7. Proposed models for *P. falciparum* gametocyte development.
Fig. S8. Flow chart of samples used in Figs. 1 to 3.
Table S1. Gametocyte fraction in bone marrow versus clinical parameters.
Table S2. Primer pairs used in qRT-PCR assay.
References (26–29)

Author contributions: R.J., S.K.N., M.T.D., T.E.T., D.A.M., and M.M. designed the experiments in this study. R.J. performed all immunohistochemistry, qRT-PCR, and ultrastructural experiments on tissue samples. S.K.N., S.D., and E.E. performed in vitro erythroid culture experiments. L.B. and P.A. performed in vitro ultrastructural experiments. J.M., K.B.S., T.E.T., and D.A.M. carried out the autopsy case and severe malaria studies in Blantyre, Malawi. B.M. and K.C.W. gave technical support on antibody optimization. R.J., S.K.N., and M.M. wrote the manuscript with input from all co-authors.

Abstract

Transmission of *Plasmodium falciparum* malaria parasites requires formation and development of gametocytes, yet all but the most mature of these sexual parasite forms are absent from the blood circulation. We performed a systematic organ survey in pediatric cases of fatal malaria to characterize the spatial dynamics of gametocyte development in the human host. Histological studies revealed a niche in the extravascular space of the human bone marrow where gametocytes formed in erythroid precursor cells and underwent development before reentering the circulation. Accumulation of gametocytes in the hematopoietic system of human bone marrow did not rely on cytoadherence to the vasculature as does sequestration of asexual-stage parasites. This suggests a different mechanism for the sequestration of gametocytes that could potentially be exploited to block malaria transmission.

INTRODUCTION

Plasmodium falciparum causes the most severe form of malaria, with almost 1 million deaths every year (1). The pathology of the disease can be attributed to the asexual stage of the parasite's life cycle, which resides within red blood cells. A small subset of parasites develops into male and female sexual forms called gametocytes that undergo maturation into gametes and then fertilization after transmission to a mosquito vector. This bottleneck in the parasite's life cycle represents an important target for intervention strategies. Only mature gametocytes are present in the human blood circulation, whereas the 6 to 8 days of immature gametocyte development takes place in tissue. The ability to be sequestered is of fundamental importance for both sexual- and asexual-stage parasites as a way to avoid clearance by the spleen. Sequestration of asexual-stage infected red blood cells (iRBCs) involves receptor-specific endothelial cytoadherence and contributes to the severe pathogenesis of *P. falciparum* malaria. In contrast, little is known about the molecular mechanisms underlying gametocyte sequestration because due to the unique maturation process of *P. falciparum* gametocytes, rodent models cannot be used to study this process. Autopsy case studies performed between 1900 (2) and the 1930s (3) and more recent analyses of biopsies and aspirates (4, 5) have revealed the presence of immature gametocytes in the bone marrow and the spleen of infected individuals. Furthermore, parasites including gametocytes have been observed in the extravascular environment of the bone marrow in human case studies (4, 6). Investigations of receptor-ligand interactions have shown negligible levels of both receptor binding (7, 8) and parasite ligand expression (9) in gametocytes, suggesting that the mechanisms involved in sequestration of developing gametocytes are distinct from the binding interactions described in asexual stages. In addition, it has recently been shown in *P. falciparum* that immature gametocyte-iRBCs are more rigid than those infected by mature gametocytes, suggesting that cell mechanical properties may be involved in the dynamics of sexual-stage sequestration (10, 11).

Here, we present the results of a systematic organ survey using autopsy cases from children who died from malaria (12) (table S1) to identify and characterize tissue sites of gametocyte accumulation.

RESULTS

To determine anatomical sites of gametocyte enrichment, we applied an immunohistochemical labeling approach using antibodies against *P. falciparum* lactate dehydrogenase (pLDH) to detect all parasites (13), and the gametocyte antigen Pfs16 (14) to detect all gametocytes (Fig. 1A and figs. S2 and S3). In the initial screen of six autopsy cases, we surveyed tissue specimens from eight organs and the subcutaneous fat. The spleen, brain, heart, and gut revealed the highest total parasite densities (Fig. 1B), which is consistent with previous studies showing high levels of asexual parasite sequestration in these organs (13, 15). Likewise, gametocyte levels were high in the spleen, brain, and gut but also in the bone marrow (Fig. 1B and fig. S1). To normalize for differences in parasite load in tissues because of heterogeneous vascularity across organs, we calculated gametocyte enrichment as the number of Pfs16-positive cells divided by the number of pLDH-positive cells for each tissue sample (Fig. 1C). This analysis revealed a significant difference in gametocyte fraction across organs ($P = 0.033$, Fisher's exact test), and an enrichment of gametocytes in the bone marrow, with a median gametocyte fraction of 44.9%, compared to 12.4% in gut, 4.8% in brain, and 3.3, 1.3, 1.3, and 0.5% in fat, lung, heart, and spleen, respectively (Fig. 1C). We were able to detect this difference despite large heterogeneity in our patient population in terms of malaria infection dynamics. The length of time between patient admission and death was associated with higher gametocyte fraction in the bone marrow, as expected, because of both natural infection dynamics (gametocyte development is triggered late in disease progression) and the differential effects of the intravenous quinine that is given to all admitted patients (quinine rapidly reduces asexual parasitemia but is less effective against gametocytes) (table S1 and Fig. 1D).

To determine whether the bone marrow is enriched for immature gametocytes (those developing stages usually absent from the peripheral circulation), we measured three gametocyte genes via mRNA expression that were shown to peak at different points along gametocyte development (16) (figs. S4 and S5 and table S2). Gene expression was measured by real-time quantitative reverse transcription polymerase chain reaction (qRT-PCR) in the spleen, brain, heart, gut, and bone marrow of five patients, the tissues with the highest gametocyte burden by immunohistochemistry. The housekeeping gene PF08_0085, *ubiquitin-conjugating enzyme* (*UCE*) was the highest transcript detected across all organs except for the bone marrow, where the young gametocyte marker *PF14_0748* was the highest transcript detected (Fig. 1E). The mean expression of both immature gametocyte markers *PF14_0748* and *Pf4845* was highest in the bone marrow, whereas the mature gametocyte marker *Pfs25* was low across all organs, which was expected given that mature gametocytes do not sequester in tissues. These data suggest that the early stages of gametocyte development are enriched within the bone marrow.

To determine the spatial distribution of parasites within the bone marrow, we performed colabeling of bone marrow sections with markers for all parasites (pLDH), gametocytes (Pfs16), and host vasculature (CD31). For this investigation, we expanded the total number of cases examined to 30 patients (Fig. 1F and fig. S8) and focused our analysis on the bone marrow from these autopsy cases. We first assessed whether sequestered gametocytes could be found associated with endothelial cells in the bone marrow, analogous to what is

described for the adherence of asexual parasite stages. Consistent with previous studies, pLDH-labeled asexual ring and schizont stages were found within the microvasculature, sometimes in close apposition to endothelial cells (Fig. 2A). In contrast, very few Pfs16-positive gametocytes were found within the blood vessels of the bone marrow. The mean fraction of gametocytes found in the microvascular compartment across patients was only 3% (Fig. 2B). Pfs16-labeled gametocytes of various stages, including small oat-shaped young gametocytes and larger oblong forms, were instead almost exclusively found in the extravascular space of the bone marrow, where they represented a mean of 48% of total parasites (Fig. 2, C and D). The difference between the proportions in the intra- versus extravascular space was significant ($P < 0.0001$, Mann-Whitney test).

Because we frequently detected hemozoin malaria pigment within macrophages in the extravascular space of the bone marrow, in agreement with a previous observation (6), we examined colocalization of parasites with the macrophage marker CD163 to investigate phagocytosis by bone marrow macrophages. We used the same cohort as the CD31 analysis but only reanalyzed the cases for which at least two pLDH-positive parasites were quantified in the previous screen. We observed that across these 22 cases, just 25% of parasites found within macrophages were gametocytes, compared with a mean gametocyte fraction of 63% that did not colocalize with macrophages. The difference between the gametocyte fractions inside versus outside macrophages was significant ($P = 0.0169$, Mann-Whitney test). These results suggest that sexual stages are less susceptible to phagocytosis during development than asexual stages (Fig. 2, E and F), a finding that is consistent with previous in vitro data (17). Together, these findings suggest that immature gametocytes preferentially accumulate in the extra-vascular space of the bone marrow, where they may be partially protected from phagocytosis (although this observation may have been influenced by the greater sensitivity of asexual stages to antimalarial drugs).

To further characterize this environment, we performed an ultra-structural analysis of a bone marrow sample with a gametocyte fraction of 45%, as determined by immunohistochemistry. This analysis revealed a subset of parasites (three of four observed) with morphological features characteristic of early gametocytes, including the lack of host cell modifications, the presence of multiple food vacuoles containing hemozoin crystals, and empty remnants of RBC membrane (Fig. 2, G and I). Some of these parasites could be found adjacent to erythroid precursor cells (Fig. 2G). In the same patient, we identified parasites with classic ultrastructure of cytoadherent asexual stages (Fig. 2H).

To follow up on our ultrastructural findings, we used immunohistochemistry to investigate whether gametocytes were enriched at erythroblastic islands, clusters of nucleated erythroblasts that adhere to a “nursing” macrophage during RBC development. Islands could be readily identified in the bone marrow by labeling with an antibody against the erythroid precursor marker, transferrin receptor (CD71). We quantified the colocalization of CD71 and Pfs16 in the 8 (of 22) patients with the highest gametocyte load in bone marrow and found that across patients, 50 to 90% of all gametocytes were in contact with erythroblastic islands (Fig. 3, A and B). This enrichment was not simply the result of an overabundance of erythroid cells in the marrow; the percent of erythroid cells (as determined by myeloid to erythroid ratio) was between 20 and 50% in the same patients. Despite the frequent

association of gametocytes with erythroblastic islands, we observed only a small fraction of gametocytes (0 to 6%) within $CD71^+$ erythroid precursor cells (Fig. 3, C and D). We followed up with a size analysis in the case with the largest percentage of gametocytes in $CD71^+$ cells (6%) and found that most stage I–sized gametocytes were within $CD71^+$ cells, whereas most stage II/III–sized gametocytes were within $CD71^-$ cells (Fig. 3D, right graph). The enrichment of stage I–sized versus stage II/III–sized gametocytes in $CD71^+$ cells was significant ($P = 0.0302$, Fisher's exact test). These data show that small-sized gametocytes can be found in $CD71^+$ RBC precursor cells, and suggest that gametocytes may form in these cells and continue to develop as the host cell matures and loses CD71 surface expression. This scenario is consistent with previous evidence that gametocyte formation is enhanced in reticulocyte-enriched blood (18, 19) and that asexual *P. falciparum* can invade and develop within orthochromatic erythroblasts (20).

To directly test whether gametocytes can form in erythroid precursor cells, we used an ex vivo erythropoiesis system to generate orthochromatic erythroblasts and reticulocytes from hematopoietic stem cells (21) and incubated these with *P. falciparum* schizonts under conditions that promote gametocyte formation (fig. S6). Within the first 30 hours of parasite development, we observed gametocytes in both orthochromatic erythroblasts and reticulocytes (Fig. 3, E and F). After 5 days, most gametocytes were found in enucleated cells, reflecting the typical rate of enucleation during ex vivo erythropoiesis. These findings directly demonstrate that gametocyte formation can occur in erythroblasts and reticulocytes, as suggested by indirect evidence in a recent study (18). The experiments also corroborate our histological observations of an enrichment of small-sized gametocytes within erythroid precursors in the bone marrow.

DISCUSSION

We present evidence for the development of gametocytes in the hematopoietic system of the human bone marrow. Whereas this study was performed on autopsies from children who succumbed to clinical cerebral malaria, independent evidence for bone marrow enrichment of immature gametocytes comes from a recent study of children with nonfatal malarial anemia (22). Further studies are required to determine whether other tissues of the reticuloendothelial system such as spleen and liver can also support gametocyte development.

In addition to the enrichment in bone marrow observed histologically, we have demonstrated that gametocytes can form and develop in erythroid precursor cells. We have also shown that they are specifically enriched in the bone marrow's extravascular compartment. Developing gametocytes may be retained in the extravascular space through a binding interaction with erythroblastic islands and/or through their increased rigidity, and are rarely phagocytosed. Once mature, gametocytes may be released back into the circulation through the recently described switch in cellular deformability occurring during final gametocyte maturation (10, 11) (fig. S7). This model is fundamentally different from the established vascular cytoadherence mechanism utilized by asexual iRBCs. Identification of the hematopoietic system as a specialized niche for *P. falciparum* gametocyte development provides a rational basis for targeted mechanistic studies and for the development of new

transmission blocking interventions tailored to interrupt the hematopoietic sequestration process of the parasite.

MATERIALS AND METHODS

Study design

Given previous evidence for the presence of *P. falciparum* gametocytes in the bone marrow and spleen, we aimed to rigorously test whether these stages indeed show a tissue-specific sequestration pattern. For this purpose, we performed a systematic organ screen using existing autopsy cases of fatal malaria (12). We included the most recent cases, excluding those with HIV comorbidity, an incomplete set of archived tissues, or insufficient tissue quality as evaluated by CD31 immunohistochemistry and an RNA bioanalyzer. Parasite and gametocyte load were assessed across organs by immunohistochemistry (10 cases) and qRT-PCR (6 cases). Slides were blinded to patient ID and independently counted by two microscopists. Following up on the results of the organ screen, we further characterized the localization of parasites and gametocytes within the bone marrow. We expanded our survey to the entire autopsy cohort, excluding again those with HIV comorbidity, lack of an archived bone marrow sample, or long postmortem interval (PMI) (used as a proxy for tissue quality). This selection resulted in a total of 30 autopsy case bone marrow samples for which we colocalized host cells and parasites/gametocytes by immunohistochemistry. Following up on the results of the bone marrow characterization, we tested whether gametocytes can form in the hematopoietic environment in vitro. We performed parasite invasion experiments in which we evaluated the growth and development of parasites and gametocytes into erythroid precursor cells.

Autopsy cohort

The institutional review boards (IRBs) at the University of Malawi College of Medicine, Michigan State University, and the Harvard School of Public Health approved all aspects of the autopsy cohort study and the severe malaria cohort study. Informed written consent was obtained from all parents/guardians of the enrolled patients. IRB at the Brigham and Women’s Hospital approved the use of discarded surgical tissue for laboratory experiments.

The autopsies analyzed in this study are part of a pediatric severe malaria and postmortem autopsy study that was performed between 1996 and 2011(12). Children meeting the clinical case definition of cerebral malaria, as well as controls with parasites, were admitted to the Malaria Research Ward, located in the Queen Elizabeth Central Hospital in Blantyre, Malawi, and enrolled in the severe malaria study upon the consent of the parent or guardian. Criteria used for diagnosis and clinical management have been previously described (12). More than 2000 individuals were enrolled in the study over this time period. The mortality rate for the study participants was between 15 and 20%. Consent was given to conduct an autopsy for 103 cases, and these autopsies were performed between 2 and 14 hours after death.

Tissue specimens were collected in various formats at the time of autopsy. Specimens were stored in 10% neutral buffered formalin to be later used for immunohistochemical analysis,

stored in glutaraldehyde buffer for electron microscopy, and snap-frozen in RNAlater (Qiagen) for qRT-PCR analysis.

Autopsy tissues used in each analysis

For an initial screen of sites of gametocyte enrichment, we identified autopsy cases in which tissues from nine sites of interest were collected in formalin-fixed, paraffin-embedded (FFPE) tissues. On the basis of research demonstrating that HIV infection appears to accelerate the course of malaria infection and may inhibit normal human cellular immune responses (that is, macrophage clearance in the spleen) (23), we opted to exclude HIV-positive individuals or individuals of unknown status (this excluded 27% of study enrollees). Starting with the 13 most recent HIV-negative cases for which there was a tissue sample available for all nine organs in our screen (spleen, heart, brain, lung, liver, bone marrow, gut, kidney, and subcutaneous fat), we assessed tissue quality by performing immunohistochemistry using platelet endothelial cell adhesion molecule (CD31), a marker of host endothelial vessels on the spleen, heart, and bone marrow sections of each patient. Of those 13, CD31 labeling failed in at least one of these tissues in 3 cases, which we then excluded from further analysis. Among these three excluded cases were the two cases with the longest PMIs (and all three had PMI of 12 hours or longer). This left us with 10 HIV-negative, CD31-positive autopsy cases on which we performed our organ screen. These cases had PMIs ranging from 4 to 12.25 hours. We broke the organ screen into a primary organ screen in which we analyzed all nine organs from six patients, then determined the three organs with the highest gametocytemia (spleen, brain, and bone marrow), and subsequently performed a secondary organ screen in which we analyzed just these three organs. This resulted in $n = 10$ patients for the spleen, brain, and bone marrow (for both pLDH and Pfs16), and $n = 6$ for the heart, gut, lung, fat, liver, and kidney.

For the quantitative PCR analysis, we analyzed RNA from a smaller subset of patients for which tissue specimens were stored in RNAlater (only 12 total patients for which all tissues were collected in this format). There were a total of six HIV-negative patients for which a sample was collected in RNAlater for each of the top five organs of gametocyte enrichment based on the primary immunohistochemical screen (spleen, brain, heart, gut, and bone marrow). Of these, we excluded one case with poor RNA quality (as determined by lack of clear RNA bands on the Agilent Bioanalyzer in the two organs tested: brain and bone marrow). This case had a PMI greater than 12 hours. This left us with five HIV-negative cases with sufficient RNA quality, and with PMI between 4 and 12.25 hours on which we performed our qRT-PCR analysis.

For the subsequent characterization of parasites intra- and extra-vascularly using double labeling with CD31, we expanded our cohort. Returning to the list of 75 HIV-negative patients from this autopsy study, we identified a subset of 36 patients for further analysis based on applying the following filters: (i) PMI less than 9 hours (to ensure good structural preservation of tissue sections) and (ii) availability of bone marrow FFPE block. Six of these cases were subsequently excluded from further analysis because of the lack of CD31 labeling by immunohistochemistry in the bone marrow section. For the remaining 30 CD31-positive bone marrow samples, intra- and extravascular distribution of parasites and

gametocytes was assessed. For the subsequent colocalization assessments (using CD163 and CD71), we used the 22 bone marrow specimens for which at least two pLDH-labeled parasites were detected in 50 high-power fields in the previous CD31 analysis. All 22 bone marrow specimens labeled successfully with both CD163 and CD71. An overview of the selection criteria and samples used for each of these experiments is included as fig. S8.

Statistical methods

The sample size for studies of limited human tissues as in our design makes testing for statistical significance difficult, especially for acceptable *P* values, although effects sizes are suggestive of true findings. Where appropriate, Fisher's exact tests were used to determine significance of association. Effect sizes are demonstrated in graphical form. Elsewhere, Mann-Whitney tests were used for comparisons between tissue sites. Summary statistics are reported and shown graphically. For patient clinical data, *t* tests were used to test for significant differences in clinical features in patients with high versus low gametocyte fractions. Summary statistics are reported, and significant results are shown graphically.

In vitro experiments for *P. falciparum* parasite culture and gametocyte production, as well as preparation and ultrastructural analysis of isolated gametocytes were performed as described (24, 25). To develop a working protocol and antibody specificities for immunohistochemical analysis of tissue samples, we generated FFPE control blocks containing RBCs infected with asexual and sexual parasite stages combined with surgical tissue specimens. Immunohistochemical analysis on autopsy tissue was performed with antibodies against parasite markers pLDH or BIP to detect all parasites, Pfs16 for all gametocytes, CD31 for endothelial cells, CD71 for erythroid precursor cells, and CD163 for macrophages. The stage specificity of qRT-PCR markers was validated using in vitro–derived parasites from across a time course of asexual and sexual development. qRT-PCR on tissue homogenates was performed with primers against three genes with peak transcription at early, mid, and late gametocyte development, respectively. Ultrastructural analyses were performed on a subset of in vivo tissues and parasite morphology compared with that of in vitro–derived sexual stages. Finally, cRBCs were generated as described (21) in the presence of murine stromal cells. Parasite formation and development within these cells were studied after the addition of highly synchronized late-stage *P. falciparum* parasites. A detailed description of all methods used and selection of samples used in this study (fig. S8) is available in the Supplementary Materials.

Supplementary Material

Refer to Web version on PubMed Central for supplementary material.

Acknowledgments

We thank the families of the bereaved for allowing us to conduct these autopsies. For conducting the autopsies, we thank W. Namanya, D. Kothokwa, J. Kaliwamba, and L. Mbewe (mortuary assistants), as well as S. Kamiza, C. Dzamalala, and G. Liomba (Malawian pathologists). We also thank M. Makler for providing pLDH antibodies; E. Meyer, A. Frando, A. McFadden, J. Vareta, and M. Menyere for laboratory assistance; and G. Pinkus and A. Campbell for technical advice with immunohistochemistry.

Funding: This work was supported by the U.S. NIH (M.M.: R01A1077558, T.E.T.: 5R01AI034969-14, M.T.D.: R01AI091787, K.C.W.: R01AI069314). P.A. was supported through EUFP7 grant EVIMalaR (contract no. 242095). R.J. was supported by an NIH training grant (T32 AI007535) and a Harvard Initiative for Global Health fellowship. S.K.N. is supported by a postdoctoral fellowship from the Wenner-Gren Foundations (Sweden).

REFERENCES AND NOTES

1. World Health Organization. World Malaria Report 2012. World Health Organization; Geneva: 2013.
2. Marchiafava, E.; Bignami, A. Sulle Febbri Estivo Aumnali. E. Loescher; Torino: 1894.
3. Thomson JG, Robertson A. The structure and development of *Plasmodium falciparum* gametocytes in the internal organs and peripheral circulation. Trans R Soc Trop Med Hyg. 1935; 29:31–40.
4. Farfour E, Charlotte F, Settegrana C, Miyara M, Buffet P. The extravascular compartment of the bone marrow: A niche for *Plasmodium falciparum* gametocyte maturation? Malar J. 2012; 11:285. [PubMed: 22905863]
5. Smalley ME, Abdalla S, Brown J. The distribution of *Plasmodium falciparum* in the peripheral blood and bone marrow of Gambian children. Trans R Soc Trop Med Hyg. 1981; 75:103–105. [PubMed: 7022784]
6. Wickramasinghe SN, Phillips RE, Looareesuwan S, Warrell DA, Hughes M. The bone marrow in human cerebral malaria: Parasite sequestration within sinusoids. Br J Haematol. 1987; 66:295–306. [PubMed: 3304391]
7. Rogers NJ, Hall BS, Obiero J, Targett GA, Sutherland CJ. A model for sequestration of the transmission stages of *Plasmodium falciparum*: Adhesion of gametocyte-infected erythrocytes to human bone marrow cells. Infect Immun. 2000; 68:3455–3462. [PubMed: 10816498]
8. Silvestrini F, Tibúrcio M, Bertuccini L, Alano P. Differential adhesive properties of sequestered asexual and sexual stages of *Plasmodium falciparum* on human endothelial cells are tissue independent. PLOS One. 2012; 7:e31567. [PubMed: 22363675]
9. Tibúrcio M, Silvestrini F, Bertuccini L, Sander AF, Turner L, Lavstsen T, Alano P. Early gametocytes of the malaria parasite *Plasmodium falciparum* specifically remodel the adhesive properties of infected erythrocyte surface. Cell Microbiol. 2013; 15:647–659.
10. Tibúrcio M, Niang M, Deplaine G, Perrot S, Bischoff E, Ndour PA, Silvestrini F, Khattab A, Milon G, David PH, Hardeman M, Vernick KD, Sauerwein RW, Preiser PR, Mercereau-Puijalon O, Buffet P, Alano P, Lavazec C. A switch in infected erythrocyte deformability at the maturation and blood circulation of *Plasmodium falciparum* transmission stages. Blood. 2012; 119:e172–e180. [PubMed: 22517905]
11. Aingaran M, Zhang R, Law SK, Peng Z, Undisz A, Meyer E, Diez-Silva M, Burke TA, Spielmann T, Lim CT, Suresh S, Dao M, Marti M. Host cell deformability is linked to transmission in the human malaria parasite *Plasmodium falciparum*. Cell Microbiol. 2012; 14:983–993. [PubMed: 22417683]
12. Taylor TE, Fu WJ, Carr RA, Whitten RO, Mueller JS, Fosiko NG, Lewallen S, Liomba NG, Molyneux ME. Differentiating the pathologies of cerebral malaria by postmortem parasite counts. Nat Med. 2004; 10:143–145. [PubMed: 14745442]
13. Genrich GL, Guarner J, Paddock CD, Shieh WJ, Greer PW, Barnwell JW, Zaki SR. Fatal malaria infection in travelers: Novel immunohistochemical assays for the detection of *Plasmodium falciparum* in tissues and implications for pathogenesis. Am J Trop Med Hyg. 2007; 76:251–259. [PubMed: 17297032]
14. Eksi S, Williamson KC. Protein targeting to the parasitophorous vacuole membrane of *Plasmodium falciparum*. Eukaryot Cell. 2011; 10:744–752. [PubMed: 21498641]
15. Seydel KB, Milner DA Jr, Kamiza SB, Molyneux ME, Taylor TE. The distribution and intensity of parasite sequestration in comatose Malawian children. J Infect Dis. 2006; 194:208–215. [PubMed: 16779727]
16. Young JA, Fivelman QL, Blair PL, de la Vega P, Le Roch KG, Zhou Y, Carucci DJ, Baker DA, Winzeler EA. The *Plasmodium falciparum* sexual development transcriptome: A microarray analysis using ontology-based pattern identification. Mol Biochem Parasitol. 2005; 143:67–79. [PubMed: 16005087]

17. Healer J, Graszynski A, Riley E. Phagocytosis does not play a major role in naturally acquired transmission-blocking immunity to *Plasmodium falciparum* malaria. Infect Immun. 1999; 67:2334–2339. [PubMed: 10225892]
18. Peatey CL, Watson JA, Trenholme KR, Brown CL, Nielson L, Guenther M, Timmins N, Watson GS, Gardiner DL. Enhanced gametocyte formation in erythrocyte progenitor cells: A site-specific adaptation by *Plasmodium falciparum*. J Infect Dis. 2013; 208:1170–1174. [PubMed: 23847056]
19. Trager W, Gill GS, Lawrence C, Nagel RL. *Plasmodium falciparum*: Enhanced gametocyte formation in vitro in reticulocyte-rich blood. Exp Parasitol. 1999; 91:115–118. [PubMed: 9990338]
20. Tamez PA, Liu H, Fernandez-Pol S, Haldar K, Wickrema A. Stage-specific susceptibility of human erythroblasts to *Plasmodium falciparum* malaria infection. Blood. 2009; 114:3652–3655. [PubMed: 19706885]
21. Giarratana MC, Rouard H, Dumont A, Kiger L, Safeukui I, Le Pennec PY, François S, Trugnan G, Peyrard T, Marie T, Jolly S, Hebert N, Mazurier C, Mario N, Harmand L, Lapillonne H, Devaux JY, Douay L. Proof of principle for transfusion of in vitro–generated red blood cells. Blood. 2011; 118:5071–5079. [PubMed: 21885599]
22. Aguilar R, Magallon-Tejada A, Achtman AH, Moraleda C, Joice R, Cisteró P, Li Wai Suen CS, Nhabomba A, Macete E, Mueller I, Marti M, Alonso PL, Menéndez C, Schofield L, Mayor A. Molecular evidence for the localization of *Plasmodium falciparum* immature gametocytes in bone marrow. Blood. 2014; 123:959–966. [PubMed: 24335496]
23. Flateau C, Le Loup G, Pialoux G. Consequences of HIV infection on malaria and therapeutic implications: A systematic review. Lancet Infect Dis. 2011; 11:541–556. [PubMed: 21700241]
24. Fivelman QL, McRobert L, Sharp S, Taylor CJ, Saeed M, Swales CA, Sutherland CJ, Baker DA. Improved synchronous production of *Plasmodium falciparum* gametocytes in vitro. Mol Biochem Parasitol. 2007; 154:119–123. [PubMed: 17521751]
25. Silvestrini F, Lasonder E, Olivieri A, Camarda G, van Schaijk B, Sanchez M, Younis Younis S, Sauerwein R, Alano P. Protein export marks the early phase of gametocytogenesis of the human malaria parasite *Plasmodium falciparum*. Mol Cell Proteomics. 2010; 9:1437–1448. [PubMed: 20332084]
26. van der Loos CM. Multiple immunoenzyme staining: Methods and visualizations for the observation with spectral imaging. J Histochem Cytochem. 2008; 56:313–328. [PubMed: 18158282]
27. Daily JP, Scanfeld D, Pochet N, Le Roch K, Plouffe D, Kamal M, Sarr O, Mboup S, Ndir O, Wypij D, Levasseur K, Thomas E, Tamayo P, Dong C, Zhou Y, Lander ES, Ndiaye D, Wirth D, Winzeler EA, Mesirov JP, Regev A. Distinct physiological states of *Plasmodium falciparum* in malaria-infected patients. Nature. 2007; 450:1091–1095. [PubMed: 18046333]
28. Sinden RE. Gametocytogenesis of *Plasmodium falciparum* in vitro: Ultrastructural observations on the lethal action of chloroquine. Ann Trop Med Parasitol. 1982; 76:15–23. [PubMed: 7044323]
29. Cranston HA, Boylan CW, Carroll GL, Sutera SP, Williamson JR, Gluzman IY, Krogstad DJ. *Plasmodium falciparum* maturation abolishes physiologic red cell deformability. Science. 1984; 223:400–403. [PubMed: 6362007]

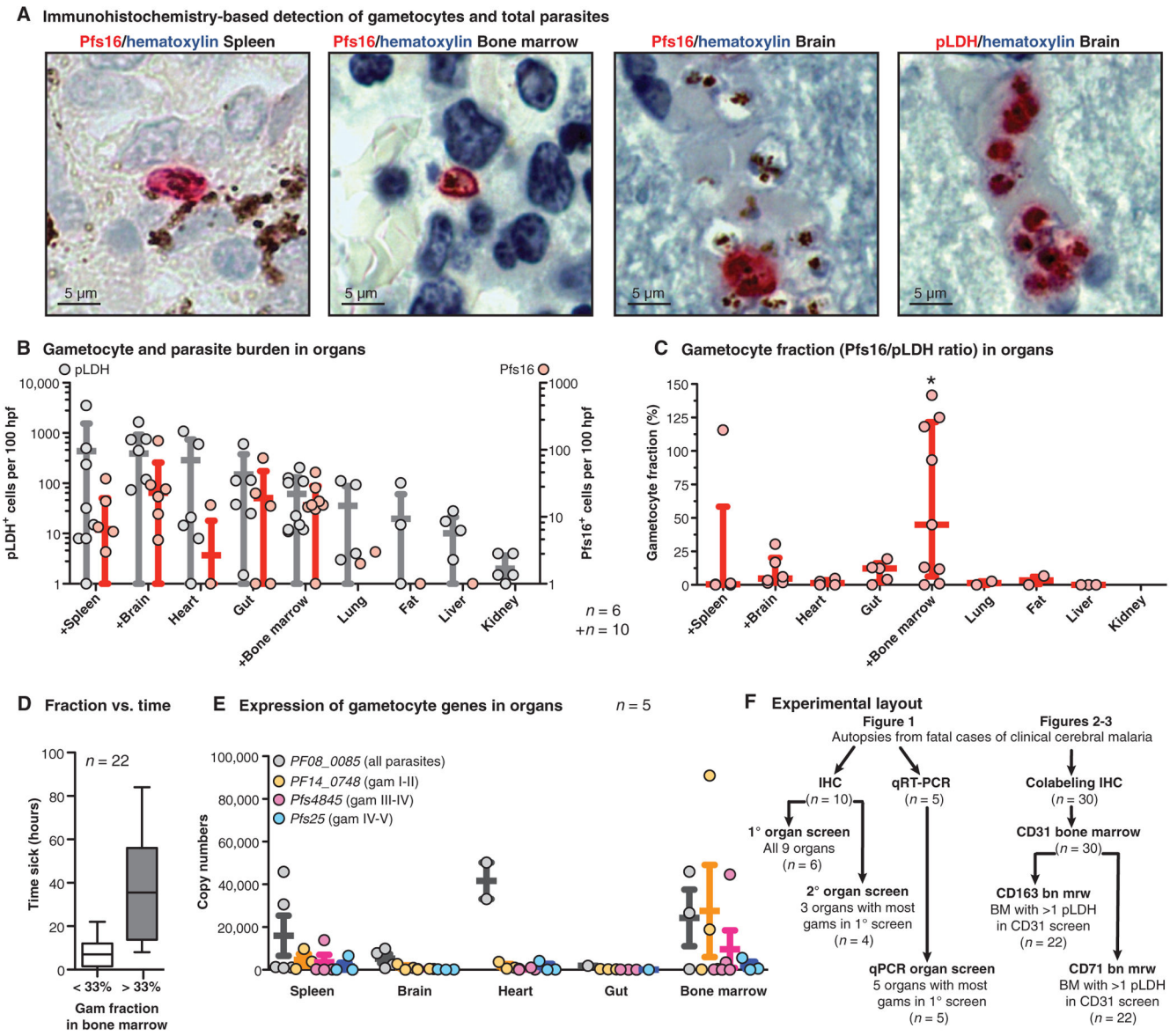

Fig. 1. Enrichment of developing gametocytes in the human bone marrow

(**A**) Detection of parasites and gametocytes across tissues. Parasite antigens (pLDH for all parasites and Pfs16 for gametocytes) were visualized with alkaline phosphatase and Fast Red substrate, and nuclei were labeled with blue hematoxylin stain. Shown are representative images of Pfs16-labeled gametocytes in the spleen, bone marrow, and brain, and of multiple pLDH-labeled sequestering parasites in the brain microvasculature. (**B** and **C**) Quantification of parasite and gametocyte load across tissues. Numbers of pLDH-positive (left axis) and Pfs16-positive (right axis) parasites were quantified per 100 high-power fields (hpf) for each organ for 6 or 10 patients (those marked with +). Dots indicate the parasite load (one dot per patient), with bars for mean and SD across patients. Gametocyte fractions (C) were calculated as a ratio of Pfs16-positive parasites to pLDH-positive parasites in 100 high-power fields from each sample, for each tissue in which at

least 10 pLDH parasites were observed. Dots indicate gametocyte fraction in each patient, with bars for median and interquartile range across patients. Asterisk above graph indicates significant difference by Fisher's exact test using categories of <33% and >33% gametocyte fraction and comparing the top five organs. (**D**) Distribution of time to death compared with gametocyte fraction. The time (hours) from admission to death for all patients from which the bone marrow gametocyte fraction was calculated in this study, plotted by those cases with gametocyte fractions below and above 33%. (**E**) Gametocyte-stage distribution across tissues by qRT-PCR. Transcript copy number for early developing (stage I/II, *PF14_0748*), mid developing (stage III/IV, *Pfs4845*), and late developing and mature gametocytes (stage IV/V, *Pfs25*) and the constitutive marker *PF08_0085* in tissue homogenates, normalized by RNA input. RNA from five organs was analyzed from five patients. Dots indicate transcript copy number in each patient, with bars for mean and SE. (**F**) Summary of the autopsy cases and experimental methods used in this study. IHC, immunohistochemistry.

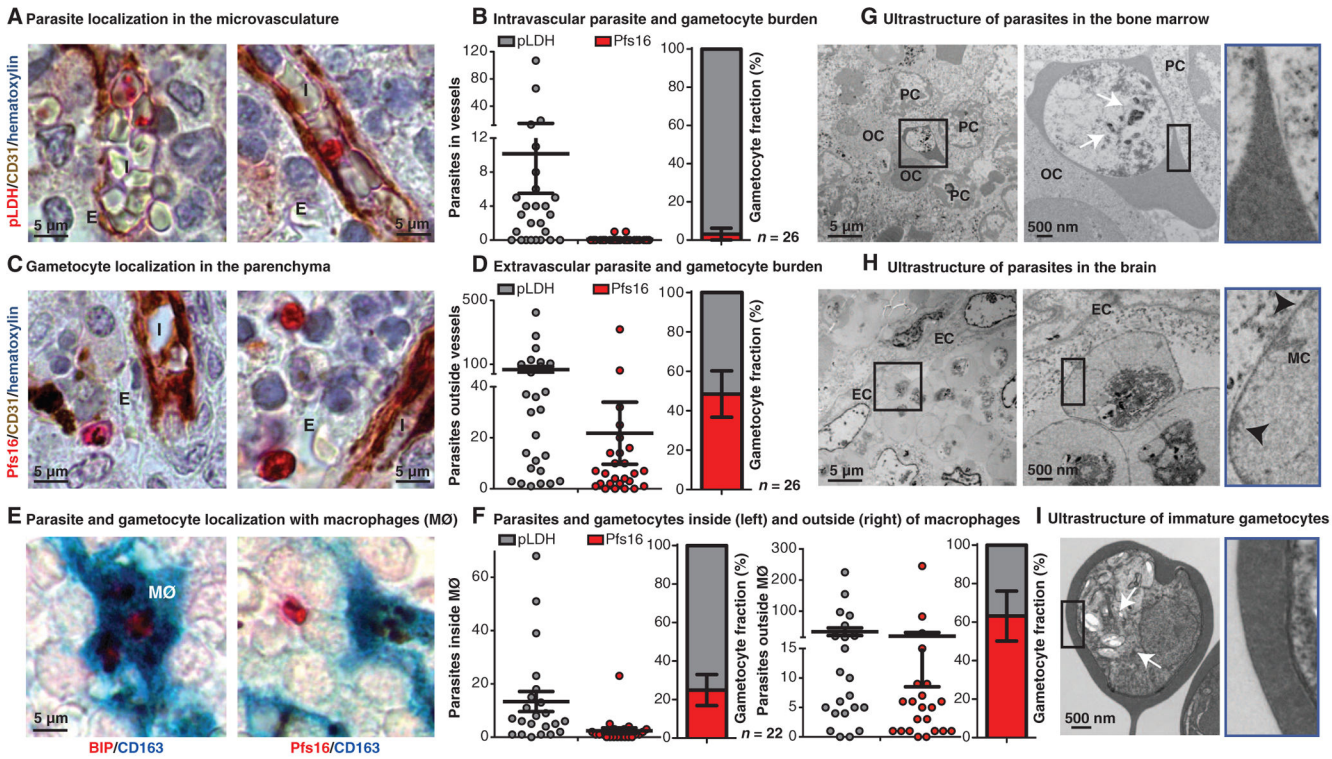

Fig. 2. Presence of gametocytes in the hematopoietic system

(**A** and **C**) Gametocyte and parasite localization in human bone marrow. Parasite antigens were detected using alkaline phosphatase and Fast Red, endothelial cells were labeled with CD31 antibodies and detected with horseradish peroxidase (HRP) and 3,3′-diaminobenzidine (DAB) chromogen, and nuclei were labeled with blue hematoxylin stain. In representative images from one patient, ring stage (top left) and large adhering trophozoite or schizont stage (top right), parasites can be seen within bone marrow sinusoids intravascularly (I). Pfs16-labeled gametocytes can be seen in the extravascular space (E). (**B** and **D**) Quantification of bone marrow vasculature localization for Pfs16- and pLDH-positive cells. Number of pLDH- and Pfs16-labeled parasites was plotted for 50 sinusoids (intravascular) (B) or 50 high-power fields of extravascular space (D) for 30 patients (only 26 had any detectable parasites by immunohistochemistry). Mean gametocyte fractions with SE across 26 patients for intravascular (3.13 ± 3.13%) and extravascular (48.49 ± 11.74%) localization are shown. (**E**) Parasite and gametocyte localization within macrophages. Pfs16 and the constitutive parasite marker BIP/heat shock protein 70 were detected using alkaline phosphatase and Fast Red substrate, and macrophages (MØ) were labeled with CD163 antibodies and detected using HRP and 3,3′,5,5′-tetramethylbenzidine (TMB) substrate (turquoise). Multiple asexual schizont stages were seen within a macrophage (left), and a gametocyte is seen outside of macrophages within the bone marrow. (**F**) Quantification of bone marrow macrophage localization for Pfs16- and pLDH-positive cells. Shown are numbers of pLDH- and Pfs16-labeled parasites in 200 macrophages, either inside macrophages (left graph) or 50 high-power fields of extracellular space outside the macrophages (right graph) for 22 patients [those cases with more than two parasites in (D)]. Mean gametocyte fraction and SE from 22 patients for inside (24.94 ± 8.03%) and outside

(63.22 ± 12.97%) macrophages. (**G** to **I**) Ultrastructural analysis of asexual and sexual parasites. Transmission electron micrograph images from the bone marrow and brain tissue samples of one patient and in vitro–derived purified stage I/II gametocytes for reference were analyzed. In the bone marrow, large knobless parasites were found in close association with multiple orthochromatic (OC) and polychromatic (PC) erythroid precursor cells (G). For comparison, sequestered asexual parasites with electron-dense knob structures (black arrowheads) and host modifications [Maurer's clefts (MC)] were observed in brain capillaries, in close apposition to endothelial cells (EC) (H). Parasites found in the bone marrow shared key features with in vitro–derived stage I gametocytes, including multiple food vacuoles with hemozoin crystals (white arrows) and lack of knobs (I).

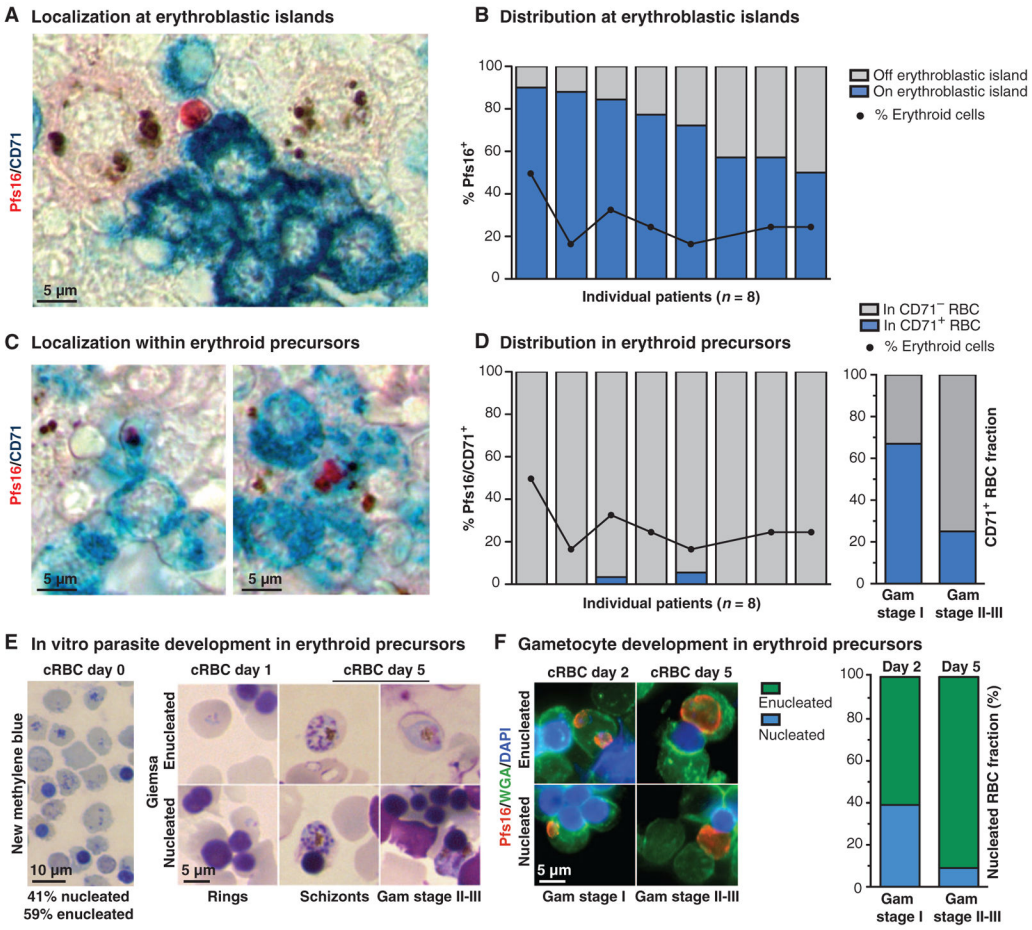

Fig. 3. Gametocyte formation and development within the hematopoietic system

(**A** and **C**) Gametocyte localization with erythroid precursor cells in the human bone marrow. Pfs16 was detected using alkaline phosphatase and Fast Red, and erythroid precursor cells were labeled with CD71 antibodies and detected with HRP and TMB liquid substrate (turquoise). Gametocytes were seen in contact with $CD71^+$ cells within an erythroblastic island (A) and within $CD71^+$ cells (C). (**B** and **D**) Quantification of gametocyte localization with erythroid precursor cells. The percentage of all gametocytes quantified in 50 high-power fields that were in contact with $CD71^+$ cells and/or the central macrophage of an erythroblastic island. The percentage of erythroid cells (as opposed to myeloid cells) is plotted for reference. Data are shown for the eight patients with the highest gametocyte load (above five gametocytes in 50 high-power fields); each bar represents one patient. A focused analysis on the gametocytes in the patient with the highest fraction of gametocytes in $CD71^+$ cells is shown (D, right graph). The proportion of gametocytes within $CD71^+$ cells for stage I size versus stage II to III size is shown. Gametocyte sizes as determined using ImageJ were assigned to either stage I or stage II/III on the basis of comparison with in vitro stage measurements (fig. S3). For this analysis, 15 gametocytes were measured from each category ($CD71^+$, $CD71^-$). (**E** and **F**) In vitro parasite development in erythroid precursor cells. Cultured RBCs (cRBCs) were stained with new methylene blue to assess erythroid maturation (presence of nucleus or ribosomal RNA) on

day 0 (E, left panel). Giemsa-stained smears of infected cRBCs on days 1 and 5 demonstrate asexual development and replication, as well as gametocyte development within these cells (E, right panel). For gametocyte detection, parasites were labeled with Pfs16 antibodies (red), RBC precursors were stained with wheat germ agglutinin (WGA; green), and nuclei were stained with 4′,6-diamidino-2-phenylindole (DAPI; blue). The distribution of host cell type is shown for each gametocyte-stage category, morphologically identified by size and shape of Pfs16-labeled cells.